Monitoring energy efficiency of condensing boilers via hybrid first-principle modelling and estimation

Satyavada, Harish; Baldi, Simone

DOI
10.1016/j.energy.2017.09.124

Publication date
2018

Document Version
Final published version

Published in
Energy

Energy 142 (2018) 121–129

Contents lists available at ScienceDirect

Energy

journal homepage: www.elsevier.com/locate/energy

Monitoring energy efficiency of condensing boilers via hybrid first-principle modelling and estimation☆

Harish Satyavada [a], Simone Baldi [b, *]

[a] General Electric Global Research, Whitefield, Bangalore, India
[b] Delft Center for Systems and Control, Delft University of Technology, Delft, The Netherlands

ARTICLE INFO

Article history:
Received 23 February 2017
Received in revised form
14 September 2017
Accepted 25 September 2017
Available online 13 October 2017

Keywords:
Hybrid modelling
State-dependent switching
Dynamic monitoring
Condensing boiler
Multiple-model estimation

ABSTRACT

The operating principle of condensing boilers is based on exploiting heat from flue gases to pre-heat cold water at the inlet of the boiler: by condensing into liquid form, flue gases recover their latent heat of vaporization, leading to 10–12% increased efficiency with respect to traditional boilers. However, monitoring the energy efficiency of condensing boilers is complex due to their nonlinear dynamics: currently, (static) nonlinear efficiency curves of condensing boilers are calculated at quasi-stationary regime and 'a posteriori', i.e. from data collected during chamber tests: therefore, with this static approach, it is possible to monitor the energy efficiency only at *steady-state* regime. In this work we propose a novel model-based monitoring approach for condensing boilers that extends the operating regime for which monitoring is possible: the approach is based on a hybrid dynamic model of the condensing boiler, where state-dependent switching accounts for dynamically changing condensing/non condensing proportions. Monitoring the energy efficiency over the boiler's complete *dynamic regime* is possible via switching estimators designed for the different condensing/non condensing modes. By using real-world boiler efficiency data we show that the proposed approach results in a (dynamic) nonlinear efficiency curve which gives a more complete description of the condensing boilers operation than static nonlinear efficiency curves: in addition, the dynamic curve can be derived 'a priori', i.e. from first principles, or from data collected during normal boiler operation (without requiring special chamber tests).

1. Introduction

Many reports and data confirm that in both Europe and US energy used by buildings accounts for over one third of energy consumption and CO_2 emissions [1]. Among the possible ways to improve energy efficiency in the building sector, developing better control and energy monitoring strategies can result in 10–40% energy savings [2]. The most accurate control and energy monitoring strategies are model-based: this means that mathematical models of the energy and heat transfer dynamics of the building equipment are developed and used to design better operational strategies (for energy-efficient control) or to monitor deviations of the energy consumptions from nominal patterns (for monitoring of energy efficiency). In this work we will focus on monitoring the energy efficiency of condensing boilers, which are becoming a more and more crucial equipment inside heating, ventilating and air conditioning (HVAC) systems: in fact, boiler operation has been estimated in around 85% of the HVAC energy consumption and 67% of the HVAC CO_2 emissions [3]. Nowadays condensing boilers are replacing less energy-efficient traditional boilers [4,5]. The operating principle of condensing boilers is based on exploiting heat from flue gases to pre-heat cold water at the inlet of the boiler. When flue gases condense into liquid form, they recover their latent heat of vaporization (see Fig. 1). The condensing mode can result in as much as 10–12% increase in efficiency with respect to traditional boilers. For the condensing mode to be activated, return water temperature at the boiler inlet should be low and below the dew temperature of the flue gas: when this condition is not maintained, the boiler will operate in the traditional non-condensing mode [6].

External conditions and ageing (wearing of materials, isolation,

☆ The research leading to these results has been partially funded by the Marie-Curie call FP7-PEOPLE-2012-IAPP 'Advanced Methods for Building Diagnostics and Maintenance' (AMBI).

* Corresponding author.
E-mail addresses: satyavada93@gmail.com (H. Satyavada), s.baldi@tudelft.nl (S. Baldi).

https://doi.org/10.1016/j.energy.2017.09.124

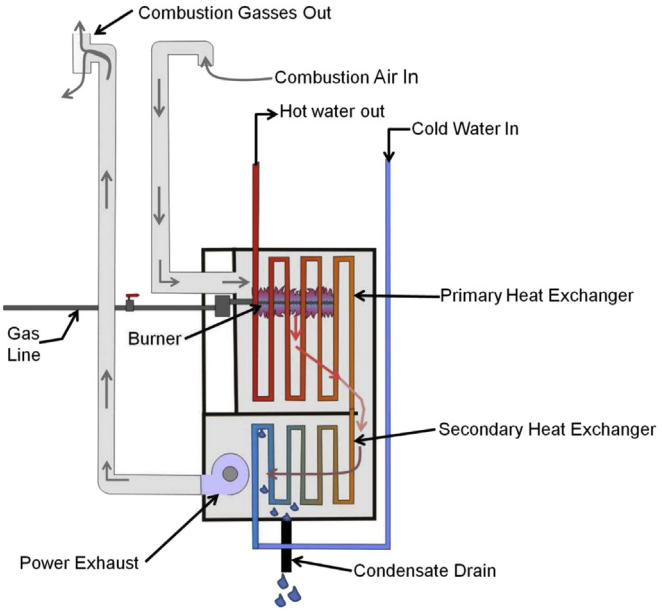

Fig. 1. Condensing boiler, retrieved from Ref. [7].

limescale, etc.) will lead to major deviations from the nominal energy efficiency of condensing boilers, thus calling for a constant monitoring of efficiency. Due to their bimodal (condensing/non-condensing) behavior, model-based monitoring of condensing boilers is more complex than model-based monitoring of traditional boilers: this is due to the complexity in modelling boiler dynamics over their entire operating range. Currently, the efficiency of condensing boilers is calculated via nonlinear efficiency curves, which are derived 'a posteriori', i.e. from data collected during special tests in adiabatic chambers, performed by the manufacturer at static or quasi-stationary regime (the interested reader can consult the technical libraries of many boiler manufacturers). However, static boiler operation in adiabatic chambers can be very different than dynamic boiler operation in buildings [8]. In other words, the range of validity of models derived from experimental tests is limited to the domain of the experimental data, which is the main limitation of the current state of the art [9]: therefore, it not appropriate to use the efficiency curve derived from static data to design monitoring strategies for dynamic regimes. New model-based monitoring methods are needed, which should be derived 'a priori', i.e. involving parameters derived from physical considerations, or from data collected during dynamic operation without requiring special chamber tests. By capturing the dynamic operation of condensing boilers instead of the static one, energy efficiency could then be monitored in the entire range of condensing boiler operation. Achieving this goal is at the core of the presented work, which overcomes the state of the art as summarized in the next section.

1.1. Related work

Mathematical models of boilers are meant to estimate the boiler efficiency as a function of certain design parameters. For traditional boilers several dynamic models have been developed, e.g. first-principle models [10,11], fuzzy models [12], Markovian jump models [13], and nonlinear models [14]. However, the situation for condensing boilers is less rich: static models of condensing boilers are dominating literature: in Refs. [15,16] the static efficiency is computed or measured as a function of the return water temperature, while in Ref. [17] the static seasonal efficiency of condensing boilers is normalized with respect to efficiency at full load. Static models are also used to calculate flue gas exit temperature and condensation rate of water vapor as a function of return water temperature: in Ref. [18] a payback period for retrofitting a conventional boiler into a condensing boiler is calculated based on static combustion and heat transfer calculations; in Ref. [19] a static model of a condensing heater is developed to evaluate the impact of relative humidity on the efficiency; Ref. [20] derives static charts for boiler combustion efficiency according to different natural gas blends characteristics parameters. On the other end of the spectrum are models based on computational fluid dynamic [21] that, due to their complexity, can be used to study new materials, but they cannot be used for real-time monitoring or control purposes [22].

The simplest way to describe some dynamical behavior of condensing boilers is the lumped element model [23], whose main limitation is assuming that the heat exchange occurs in a single point: this does not allow to differentiate between the wet exchange of condensing mode and the dry exchange of non-condensing mode. For this reason, a more common approach is to couple the lumped element model with a nonlinear efficiency curve [24]: unfortunately, as the nonlinear efficiency curve is obtained from steady-state operation, there is no guarantee that the same efficiency curve is valid also in dynamic regime: actually, the boiler efficiency during transient behavior is typically lower than at steady state [8]. The approach in Ref. [25] proposes a set of equations based on steady-state operation and two point heat exchange which describe the main physical processes inherent to the boiler sub-components; in Ref. [26] the heat transfer between the flue gases and the water is calculated by the classical ε-NTU method and a fixed distribution of dry/wet heat exchange; in Ref. [27] the dynamic behavior of the model is obtained by extending the nonlinear efficiency curve (obtained) from steady-state data with thermal mass considerations; in Ref. [28], an analytical heat transfer model in a secondary heat exchanger was proposed to calculate the heat transferred from flue gas to cooling water and the condensation rate of water vapor in the flue gas. Unfortunately, by relying on the lumped element model idea, all these approaches neglect that the heat transfer in condensing boilers is spatially distributed and time dependent: the proportion of dry/wet exchange in condensing boilers change dynamically in space and time. Furthermore, in most works mentioned above, heat transfer is considered only through water and gas, while a more complex and realistic heat exchange model should include the heat transfer via the extended surface and the tube wall. Despite the numerous modelling approaches which have been listed, we can clearly identify a series of shortcomings in existing condensing boiler models:

- Heat transfer dynamics are oversimplified to a static nonlinear efficiency curve. The efficiency curve is calculated by installers and specifiers of condensing boilers, *at steady-state* (e.g. in special adiabatic rooms). Therefore, current models are not able to capture the true heat transfer dynamics.
- The bimodal condensing/non-condensing behavior is oversimplified with two heat exchangers, one for dry and one for wet heat exchange, always in a *fixed proportion.* A model is required that can capture dynamical changes in space and time of dry/wet heat exchange.

With this work we will bridge these gaps and arrive to a novel monitoring approach. First, we exploit some preliminary ideas by the authors [29] to develop a model with state-dependent switching triggered by the temperature of the combustion gas: the switching mechanism is able to describe highly dynamic

behavior in heat transfer and distribution of dry/wet heat exchange. Then, we show that monitoring the energy efficiency over the boiler's complete *dynamic regime* is possible via switching estimators designed for the different condensing/non condensing modes. By using real-world boiler efficiency data we show that the proposed approach results in a (dynamic) nonlinear efficiency curve which gives a more complete description of the condensing boilers operation than static nonlinear efficiency curves: in addition, the dynamic curve can be derived 'a priori', i.e. from first principles, or from data collected during normal operation (without requiring special chamber tests). Due to its switching nature, the model can be suited for most of the hybrid control algorithms developed in recent years in the field of smart heating systems [16,23,30–32]. In addition, the proposed monitoring approach can potentially be combined with other space heating components, to the purpose of dynamic analysis of hybrid heat pump generators in residential [33] and district heating [34] systems. In particular, the monitoring algorithm can be integrated as a module of rule-based, model predictive control or multiobjective energy management systems to predict energy supply and demands in buildings [35–38].

The rest of the paper is organized as follows: Section 2 gives the basics of dynamic boiler operation and develops a hybrid dynamical model of the condensing boiler, while Section 3 presents the dynamic monitoring architecture. In Section 4 the results coming from real-world boiler efficiency data are presented. Section 5 concludes the work.

2. Condensing boiler operation

Let us first present the basics of condensing boiler dynamic operation. Fig. 1 highlights some of the key components of the boiler: the burner with combustion chamber, two heat exchangers (primary and secondary) and the stack. The burner's task is to mix fuel (natural gas) and oxygen and to enable combustion via an ignition device. The reaction taking place in the combustion chamber with 15% excess air is [39].

$$CH_4 + \frac{2}{0.85}O_2 + \frac{7.56}{0.85}N_2 \rightarrow CO_2 + 2H_2O + 8.89N_2 + 0.353O_2. \tag{1}$$

On the left-hand side of (1) we have methane, oxygen and nitrogen. The combustion gas are a mix of the products on the right-hand side of (1): 8.17% of CO_2 (carbon dioxide), 16.33% of H_2O (water vapor), 2.88% of O_2 (oxygen) and 72.62% of N_2 (nitrogen).

The gas right after the reaction in (1) has the same temperature as the flame (constant pressure adiabatic flame temperature): as the combustion gas moves through the heat exchanger, heat is transferred from gas to water, passing through different layers as sketched in Fig. 2. Let us identify four layers: combustion gas, extended surface, tube wall and water. The combustion gas

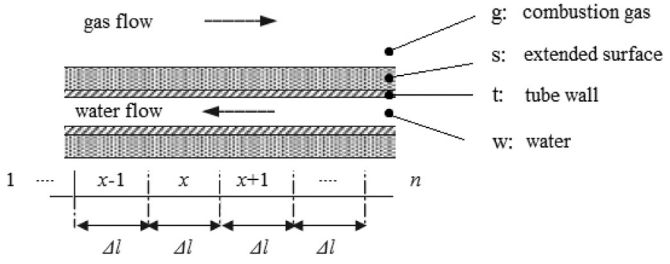

Fig. 2. Heat exchange in condensing boilers.

temperature T_g and water temperature T_w in [°C] evolve dynamically according to [40]:

$$\frac{\partial T_g}{\partial t} = -\frac{w_g}{\rho_g A_s}\frac{\partial T_g}{\partial l} - \frac{h_s D_s}{c_g \rho_g A_s}(T_g - T_s) \tag{2}$$

$$\frac{\partial T_w}{\partial t} = \frac{w_w}{\rho_w A_t}\frac{\partial T_w}{\partial l} - \frac{h_t D_t}{c_w \rho_w A_t}(T_w - T_t), \tag{3}$$

where the first term on the right-hand side of (2) comes from the heat exchange within the gas and the second term comes from the heat exchange with the extended surface at temperature T_s. In (2), c_g is the specific heat capacity in [kJ/kg°C], w_g the mass flow rate in [kg/s], and ρ_g density in [kg/m^3] of the combustion gas, respectively. The constants h_s, D_s and A_s are the surface convection coefficient in [kW/m^2 °C], the perimeter of the heat transfer surface in [m], and the free flow area in [m^2] on the gas side. The first term on the right-hand side of (3) comes from the heat exchange within water and the second term comes from the heat exchange with the tube wall at temperature T_t. In (3), c_w is the specific heat capacity in [kJ/kg°C], w_w the mass flow rate in [kg/s], and ρ_w the water density in [kg/m^3] of water, respectively. The constants h_t, D_t and A_t are the tube internal surface convection coefficient in [kW/m^2 °C], the perimeter of the heat transfer surface in [m], and the effective free flow area in [m^2] on the water side respectively. The tube wall temperature T_t and extended surface temperature T_s evolve dynamically according to [40]:

$$\frac{dT_t}{dt} = -\frac{h_t}{c_t \rho_t d_t}(T_t - T_w) - \frac{R_{ts} D_m}{c_t \rho_t d_t D_t}(T_t - T_s) \tag{4}$$

$$\frac{dT_s}{dt} = -\frac{h_s}{c_s \rho_s d_s}(T_s - T_g) - \frac{R_{ts} D_m}{c_s \rho_s d_s D_s}(T_s - T_t), \tag{5}$$

where the first term on the right-hand side of (4) comes from the heat exchange with water and the second term comes from the heat exchange with the extended surface. In (4), ρ_t is the density in [kg/m^3], c_t is the specific heat capacity in [kJ/kg°C] of the tube wall material, respectively. The constants d_t, d_s and R_{ts} and D_m are the tube wall thickness in [m], the extended surface wall thickness in [m], and the thermal resistance between tube wall and extended surface core in [kW/m^2 °C]. The first term on the right-hand side of (5) comes from the heat exchange with gas and the second term comes from the heat exchange with tube wall. In (5), ρ_s is the density in [kg/m^3], and c_s the specific heat capacity in [kJ/kg°C] of extended surface material, respectively. Similar equations as (2)–(5) have been derived by the authors in Ref. [29]: however, differently from Ref. [29], here we have further increased the flexibility of the model because the parameter D_m, which is the perimeter at the interface between tube wall and the extended surface, can be used to finely regulate (with $D_i < D_m < D_o$) the heat exchange through conduction. Note that (2)–(5) are equations related to sensible heat [41], i.e. they do not include any latent heat, as it will be explained hereafter.

2.1. Hybrid dynamics of latent heat

By spatially discretizing the partial differential equations (2) and (3) (gas and water side) we obtain ordinary differential equations. As a consequence, (4) and (5) must be spatially discretized as well: Fig. 2 shows that the four layers of the heat exchanger are discretized into n elements. The symbols T_{g_x,w_x,t_x,s_x}, $x \in 1,2 \ldots, n$ represent the temperature of gas, water, tube wall and extended surface in section x, each one modelled as a separate state. The

evolution of such temperatures in dry exchange is discretized as follows:

$$\begin{aligned}
\frac{dT_{g_x}}{dt} &= -\frac{w_g}{\rho_{g_x} A_s \Delta l}(T_{g_x} - T_{g_{x-1}}) - \frac{h_s D_s}{c_g \rho_{g_x} A_s}(T_{g_x} - T_{s_x}) \\
\frac{dT_{w_x}}{dt} &= \frac{w_w}{\rho_w A_t \Delta l}(T_{w_{x+1}} - T_{w_x}) - \frac{h_t D_t}{c_w \rho_w A_t}(T_{w_x} - T_{t_x}) \\
\frac{dT_{t_x}}{dt} &= -\frac{h_t}{c_t \rho_t d_t}(T_{t_x} - T_{w_x}) - \frac{R_{ts} D_m}{c_t \rho_t d_t D_t}(T_{t_x} - T_{s_x}) \\
\frac{dT_{s_x}}{dt} &= -\frac{h_s}{c_s \rho_s d_s}(T_{s_x} - T_{g_x}) - \frac{R_{ts} D_m}{c_s \rho_s d_s D_s}(T_{s_x} - T_{t_x})
\end{aligned} \tag{6}$$

where ρ_{g_x} in [kg/m^3] is the density of combustion gas in the element x, and Δl is the length of the element in [m]. Note that in the first equation of (6) the density ρ_{g_x} of combustion gas varies from element to element as the boiler is a constant-pressure combustion system (at atmospheric pressure). Thus, the density will change according to the ideal gas law $pV = mRT/M$, where P is the pressure of the gas in [pa = J/m^3], V is the volume of the gas in [m^3], R is the universal gas constant in [J/mol K], T is the absolute temperature of the gas in [K], m/M is the amount of substance of gas in [mol], equal to the mass m in [g] divided by the molar mass M in [g/mol]. It results that $\rho_g = m/V = pM/(RT)$. In order to take into account the counter flow nature of the condensing boiler, a backward discretization has been used in the first equation of (6), while a forward discretization has been used in the second equation of (6).

Equations in (6) are valid till the moisture en-trained in flue products as water vapor remains vaporized. The heat transfer phenomenon occurring under this condition is called dry exchange and the boiler is said to operate in non-condensing mode. Non-condensing mode occurs approximately above the dew point of the combustion gas, which is about 54.4 °C if the combustion occurs at 15% excess air [42], as the reaction (1). Below 54.4 °C, the water vapor will change phase and condense [42]. The condensation will occur at constant temperature, and in order to be sustained it is necessary that the return water temperature is low enough (in particular, lower than 54.4 °C). The heat transfer phenomenon occurring under this condition is called wet exchange and the boiler is said to operate in condensing mode. Wet exchange can be described by

$$\begin{aligned}
\frac{dT_{g_x}}{dt} &= 0 \\
\frac{dT_{w_x}}{dt} &= \frac{w_w}{\rho_w A_t \Delta l}(T_{w_{x+1}} - T_{w_x}) - \frac{h_t D_t}{c_w \rho_w A_t}(T_{w_x} - T_{t_x}) \\
\frac{dT_{t_x}}{dt} &= -\frac{h_t}{c_t \rho_t d_t}(T_{t_x} - T_{w_x}) - \frac{R_{ts} D_m}{c_t \rho_t d_t D_t}(T_{t_x} - T_{s_x}) \\
\frac{dT_{s_x}}{dt} &= -\frac{h_s}{c_s \rho_s d_s}(T_{s_x} - T_{g_x}) - \frac{R_{ts} D_m}{c_s \rho_s d_s D_s}(T_{s_x} - T_{t_x}) + \frac{W_{heat}}{c_s \rho_s d_s D_s \Delta l}
\end{aligned} \tag{7}$$

where the term W_{heat} in [kJ/s] due to phase change comes from making the first equation of (6) equal to zero

$$W_{heat} = c_g w_g (T_{g_x} - T_{g_{x-1}}) + h_s D_s \Delta l (T_{g_x} - T_{s_x}) \tag{8}$$

Because of the condensing regime, the temperature of the gases exiting the flue of a condensing boiler is typically 50–60 °C, as compared with 120–180 °C in a non-condensing boiler. Differently from the model derived by the authors in Ref. [29], the term (8) provides an extra feature, since it allows to determine the quantity of condensate as a function of the design parameters (note that not all the gas will become liquid). The quantity of condensate can be calculated from latent heat flow $W_{heat} = c_c w_c$, where c_c and m_c are the specific heat and mass flow rate of condensate. The mass of condensate can be calculated by integrating over time the mass flow rate of the condensate $w_c = W_{heat}/c_c$.

Remark 1. *The modelling approach (6)-(8) is modular in the sense that it is possible to add more or less sections n to increase or decrease modelling precision. In every section the heat exchange equations can be governed by either dry (6) or wet exchange (8), depending on the gas temperature T_{g_x} in each section. The resulting dynamical model is hybrid with state-dependent switching, thus capturing the spatial-dependent and time-dependent bimodal behavior exhibited by condensing boilers.*

Due to the monotonic properties of the temperature in a boiler (the water temperature is increasing from inlet to outlet and the gas temperature is decreasing from inlet to outlet), the boiler can work in at most $n+1$ configurations, depending on how many sections are operating in wet regime (from 0 sections to n sections). A representation of possible boiler modes as a function of the number of sections is given in Table 1: the table illustrates how the modes can go from all sections in dry exchange to all sections in wet exchange.

3. Dynamic monitoring

The hybrid model given by dry heat exchange (6) and wet heat exchange (7) and (8) can be exploited for monitoring the online possible changes in the efficiency. To this purpose, let us describe one section x, in dry or wet regime respectively, with the state-space formulation

$$\begin{aligned}
\frac{d\overline{T}_x}{dt} &= A_x^d \overline{T}_x + L_x^d \overline{d}_x + B_x^d \overline{u}_x \\
\frac{d\overline{T}_x}{dt} &= A_x^w \overline{T}_x + L_x^w \overline{d}_x + B_x^w \overline{u}_x,
\end{aligned} \tag{9}$$

where $\overline{T}_x = [T_{g_x} T_{w_x} T_{t_x} T_{s_x}]' \in \mathbb{R}^4$ is the state, $\overline{d}_x = [T_{g_{x-1}} T_{w_{x+1}}]' \in \mathbb{R}^2$ comes from neighbor sections, and $\overline{u}_x = [T_{g_0} T_{w_{n+1}}]' \in \mathbb{R}^2$ are the inputs to the boiler (only for the first and last sections) i.e. the gas temperature and return water temperature at the inlet. The matrices A_x^d, L_x^d and B_x^d, of appropriate dimensions, can be derived based on (6). The matrices A_x^w, L_x^w and B_x^w have a different structure than A_x^d, L_x^d and B_x^d, and can be derived based on (7). For example,

Table 1
Possible boiler modes as a function of the number of sections (D stands for dry or non-condensing exchange, W stands for wet or condensing exchange).

No. of sections	Modes
1	D-W
2	DD-DW-WW
3	DDD-DDW-DWW-WWW
⋮	⋮
n	$n+1$

$$A_x^d = \begin{bmatrix} -\frac{w_g}{\rho_{g_x} A_s \Delta l} - \frac{h_s D_s}{c_g \rho_{g_x} A_s} & 0 & 0 & \frac{h_s D_s}{c_g \rho_{g_x} A_s} \\ 0 & -\frac{w_w}{\rho_w A_t \Delta l} - \frac{h_t D_t}{c_w \rho_w A_t} & \frac{h_t D_t}{c_w \rho_w A_t} & 0 \\ 0 & \frac{h_t}{c_t \rho_t d_t} & -\frac{h_t}{c_t \rho_t d_t} - \frac{R_{ts} D_m}{c_t \rho_t d_t D_t} & \frac{R_{ts} D_m}{c_t \rho_t d_t D_t} \\ \frac{h_s}{c_s \rho_s d_s} & 0 & \frac{R_{ts} D_m}{c_s \rho_s d_s D_s} & -\frac{h_s}{c_s \rho_s d_s} - \frac{R_{ts} D_m}{c_s \rho_s d_s D_s} \end{bmatrix} \tag{10}$$

$$L_x^d = \begin{bmatrix} \frac{w_g}{\rho_{g_x} A_s \Delta l} & 0 \\ 0 & \frac{w_w}{\rho_w A_t \Delta l} \\ 0 & 0 \\ 0 & 0 \end{bmatrix} \tag{11}$$

while

$$A_x^w = \begin{bmatrix} 0 & 0 & 0 & 0 \\ 0 & -\frac{w_w}{\rho_w A_t \Delta l} - \frac{h_t D_t}{c_w \rho_w A_t} & \frac{h_t D_t}{c_w \rho_w A_t} & 0 \\ 0 & \frac{h_t}{c_t \rho_t d_t} & -\frac{h_t}{c_t \rho_t d_t} - \frac{R_{ts} D_m}{c_t \rho_t d_t D_t} & \frac{R_{ts} D_m}{c_t \rho_t d_t D_t} \\ \frac{2h_s}{c_s \rho_s d_s} + \frac{c_g w_g}{c_s \rho_s d_s D_s \Delta l} & 0 & \frac{R_{ts} D_m}{c_s \rho_s d_s D_s} & -\frac{2h_s}{c_s \rho_s d_s} - \frac{R_{ts} D_m}{c_s \rho_s d_s D_s} \end{bmatrix} \tag{12}$$

$$L_x^w = \begin{bmatrix} \frac{w_g}{\rho_{g_x} A_s \Delta l} & 0 \\ 0 & \frac{w_w}{\rho_w A_t \Delta l} \\ 0 & 0 \\ -\frac{c_g w_g}{c_s \rho_s d_s D_s \Delta l} & 0 \end{bmatrix}. \tag{13}$$

By putting together the $n+1$ configurations, we obtain

$$\frac{d\overline{T}}{dt} = \overline{A}_i(\theta)\overline{T} + \overline{B}_i(\theta)\overline{u}, \quad i \in \{0, 1, \ldots, n\}, \tag{14}$$

where $\overline{T} \in \mathbb{R}^{4n}$ is the collection of all temperatures in all sections, $\overline{u} = [T_{g_0} T_{w_{n+1}}]' \in \mathbb{R}^2$ are the gas temperature in the first section and the return water temperature at in the last section, and the matrices $\overline{A}_i \in \mathbb{R}^{4n \times 4n}$ and $\overline{B}_i \in \mathbb{R}^{4n \times 2}$ are derived accordingly (the effect of neighbor sections disappears after coupling the sections together). In (14), the switching from one configuration i to another is driven by T_{g_x} in the different sections. Finally, θ represents a set of parameters which is crucial to monitoring efficiency: in our case we assume that the following parameters influence efficiency.

- h_s, h_t and R_{ts} whose value might change due to limescale deposit and aging;
- w_w is also affected by limescale deposit, and most importantly, usually not measured in practice.

Limescale can build up on the water pipes of the heat exchanger and create an insulating layer which inhibits heat transfer to the water. It has been calculated that a 1 mm layer of limescale causes a 7% increase in boiler energy to meet the same heat demand, thus significantly modifying the boiler efficiency curve [43]. Limescale phenomena can be regarded as a combination of degradation of the boiler efficiency curve and changes in the mass flow rate, which have to be detected and diagnosed by the monitoring tools.

All values related to fluid properties (mass, density, specific heat capacity) and boiler dimensions (perimeter, area, volume) are assumed not to change with time: since h_s, h_t, R_{ts}, w_g and w_w appear in a linear fashion in (14), a linear-in-the-parameters estimator can be used to monitor their value [44].

$$\begin{aligned} &\frac{d\widehat{\overline{T}}}{dt} = \overline{A}_{m_i}\widehat{\overline{T}} + \left(\widehat{\overline{A}}_i(\theta) - \overline{A}_{m_i}\right)\overline{T} + \widehat{\overline{B}}_i(\theta)\overline{u} \\ &\dot{\widehat{\overline{A}}}_i(\theta) = \gamma_1 \varepsilon_i \overline{T}_x', \quad \dot{\widehat{\overline{B}}}_i(\theta) = \gamma_2 \varepsilon_i \overline{u}_x' \\ &\dot{s}_i(\theta) = \overline{A}_{m_i} s_i + \varepsilon_i\left(\overline{T}_x'\overline{T}_x + \overline{u}_x'\overline{u}_x\right), \quad \varepsilon_i = \overline{T} - \widehat{\overline{T}} - s_i \end{aligned} \tag{15}$$

where $\overline{A}_{m_i} \in \mathbb{R}^{4n \times 4n}$ are Hurwitz matrices and the different estimators are activated synchronously depending on T_{g_x} in the different sections. Other least-squares or gradient-based estimators can be used in place of (15) [44]. By comparing $\widehat{\overline{A}}_i$ and $\widehat{\overline{B}}_i$ with their nominal values, one can monitor trends in parameter changes: the proposed dynamic monitoring algorithm can be sketched as in Fig. 3, where the different estimators, one for each regime, are activated based on state-dependent conditions.

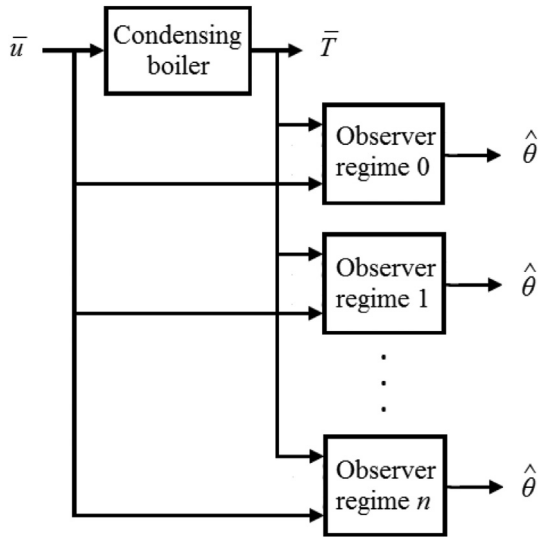

Fig. 3. Hybrid observer for condensing boiler efficiency monitoring.

3.1. Reducing the need for measurements

The monitoring algorithm in (15) exploits the underlying assumption that the entire state $\bar{T}$ can be measured. This can be quite a strong assumption, as temperatures of tube wall and extended surface might be quite difficult to measure. There are several approaches to relax this assumption. The first one is observer-based monitoring, which requires only measurements water and/or gas temperature. Consider the following descriptions of one section x in dry and wet exchange regime

$$\begin{aligned}\frac{d\bar{T}_x}{dt} &= A_x^d\bar{T}_x + L_x^d\bar{d}_x + B_x^d\bar{u}_x\\ \frac{d\bar{T}_x}{dt} &= A_x^w\bar{T}_x + L_x^w\bar{d}_x + B_x^w\bar{u}_x\\ \bar{y}_x &= C_x\bar{T}_x = \begin{bmatrix}1 & 0 & 0 & 0\\ 0 & 1 & 0 & 0\end{bmatrix}\bar{T}_x\end{aligned} \tag{16}$$

where the matrix C_x is used to isolate the measurable variables T_{g_x} and T_{w_x}. The following adaptive observer can be adopted

$$\begin{aligned}\frac{d\bar{T}}{dt} &= \bar{A}_i(\theta)\bar{T} + \bar{B}_i(\theta)\bar{u},\ \ \bar{y} = \bar{C}\bar{T},\ \ \ i\in\{0,1,\ldots,n\}\\ \frac{d\hat{\bar{T}}}{dt} &= \hat{\bar{A}}_i(\theta)\hat{\bar{T}} + \hat{\bar{B}}_i(\theta)\bar{u} + \bar{K}_i\left(\bar{y}-\hat{\bar{y}}\right),\ \ \hat{\bar{y}} = \bar{C}\hat{\bar{T}},\end{aligned} \tag{17}$$

with $\bar{C}\in\mathbb{R}^{2n\times 4n}$, $\bar{y}\in\mathbb{R}^{2n}$ collecting the measurements of gas and water temperature in all sections, and $\bar{K}_i\in\mathbb{R}^{4n\times 2n}$ has to be designed, eventually at every time step, is such a way that $(\hat{\bar{A}}_i(\theta) - \bar{K}_i\bar{C})$ is a Hurwitz matrix. Provided that the couple $(\hat{\bar{A}}_i(\theta),\bar{C})$ is detectable, using classical results from adaptive control [44], stability of the observer can be proven. If the inputs to the boiler are persistently exciting, then the estimates $\hat{\bar{A}}_i(\theta)$ and $\hat{\bar{B}}_i(\theta)$ (updated via a gradient-based algorithm) can converge to their true values.

The resulting dynamic monitoring architecture can also be sketched as in Fig. 3, where the different estimators, one for each regime, are activated based on state-dependent conditions. The activation of the different observers can be based on active measurements of the modes or on mode-identification mechanisms. Active measurements of the modes require that T_{g_x}, the state that is responsible for the switching, is measurable. This means that the number of sections under consideration cannot be greater than the number of sensors measuring T_{g_x} along the heat exchanger (at most one section for each sensor). Since measurements of water temperature are quite common in boilers, an alternative approach is to have T_{w_x} as the state that is responsible for the switching: this is motivated by the fact that nonlinear efficiency curves are given as a function of water temperature. Therefore, different sensors of water or gas temperature along the heat exchanger should be available in order to accurately identify the modes: in the absence of many sensors (e.g. in the presence of two sensors to measure inlet/outlet water temperature and a sensor to measure gas flue temperature), one should resort to mode-identification techniques, which include nonlinear estimation techniques [45,46], identification methods for hybrid systems [47,48], and estimation via multiple-models [49–51]. Note that for all these techniques, in general, a trade-off exists between available measurements and accuracy of the estimation of the active mode. Therefore, the complexity of the monitoring mechanism (the $n+1$ possible configurations) is always driven by the number of available sensors.

4. Simulation and real-world results

The efficiency of the boiler is the ratio between output power (water side) and input power (gas side): the input power P_{in} in [kW] is calculated from

$$P_{in} = w_{ng}H_v, \tag{18}$$

where w_{ng} is the mass flow rate in [kg/s] and H_v the low heating value of natural gas in [kJ/kg], respectively. The output power is given by Ref. [52]:

$$P_{out} = w_w C_w\left(T_{sup} - T_{ret}\right), \tag{19}$$

where T_{sup} in [°C] is the supply water temperature at the boiler outlet and T_{ret} in [°C] the return water temperature at the boiler inlet. As a consequence

$$\text{Efficiency} = \frac{P_{out}}{P_{in}}\cdot 100. \tag{20}$$

To draw the efficiency curve stemming from the proposed modelling approach, simulations have been performed on a MATLAB® implementation of the condensing boiler with $n = 5$ sections. The parameters w_{ng}, w_w and T_{ret} are kept constant during the simulation till steady state is reached. Then, efficiency is obtained from (20). The steady-state simulations are run over different values of T_{ret}, ranging from 20 °C to 70 °C. Fig. 4 shows the resulting efficiency curve as a function of T_{ret} for three different flow rates (w_{ng}). It can be observed that the efficiency curve resembles the typical condensing boiler efficiency curve appearing in literature [41]. Note that, as expected, greater efficiency is attained when return water temperature is below the dew point.

4.1. Comparisons with real-world efficiency curves

It is important to validate the proposed approach against real-world boilers. In order to do so, we use a CREST condensing boiler by Lochinvar, whose efficiency curve and parameters can be found in Refs. [53] and [54]. The idea is to see if the efficiency curve of the proposed model can match the efficiency of a real condensing boiler. The boiler has water volume 215 gallons (=0.814 m^3), 272 sq. ft. heating surface (=25 m^2), water mass flow rate in the range 350-45 gallon per minute (22.082–2.839 kg/s), and firing rate range 3,220,000–184,000 (Btu/h) (=944-54 [kW],

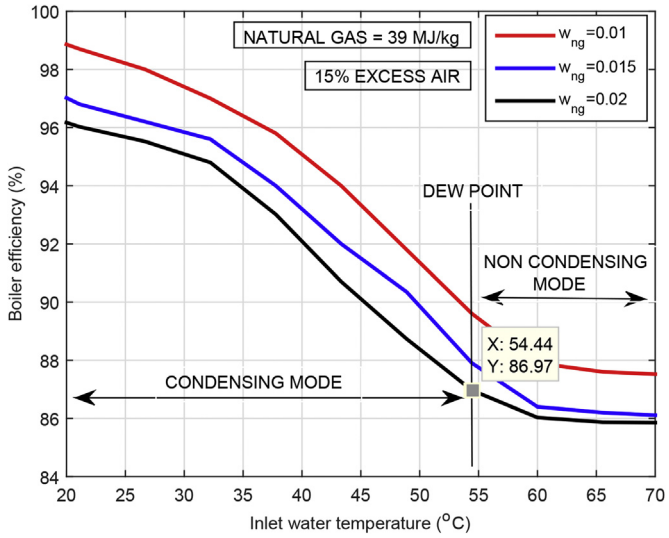

Fig. 4. Efficiency curve of the proposed model as a function of return water temperature.

which for a heating value of 55,500 kJ/kg gives approximately a methane mass flow rate of 0.0170–0.0001 kg/s). Fig. 5 shows a good match between the efficiency curves of the CREST boiler and of the proposed model. The values for the identified parameters are shown in Table 2. The error between the real efficiency curve and our proposed model is around 0.5%. To see how the accuracy of the model changes for changing number of sections, Fig. 6 shows a better match with the CREST boiler by using $n = 7$ sections. Furthermore, Fig. 7 shows that the accuracy is a decreasing function of the number of sections: in practice, increasing the number of sections also requires more sensors, in order to be able to identify all the modes in Table 1. Therefore, as explained in Section 3.1, a trade-off should be made between accuracy and available sensors.

From literature we know that steady-state efficiency can be different than transient efficiency [8]: Fig. 8 shows that, as expected, transient efficiency is lower than steady-state efficiency. Note that no state-of-the-art approach based on static nonlinear efficiency curve can provide the transient efficiency of a boiler. Therefore, Fig. 8 shows that what we gain with the proposed

Table 2
Parameter identification for CREST boiler.

Parameter	Value	Unit
w_g (low gas)	7.30×10^{-4}	[kg/s]
w_g (high gas)	1.46×10^{-2}	[kg/s]
w_w	9.64×10^{-2}	[kg/s]
ρ_g	ideal gas law	[kg/m^3]
ρ_w	988	[kg/m^3]
ρ_t	7850	[kg/m^3]
ρ_s	8940	[kg/m^3]
c_g	1.097	[kJ/kg °C]
c_w	4.18	[kJ/kg °C]
c_t	0.49	[kJ/kg °C]
c_s	0.39	[kJ/kg °C]
D_s	0.24	[m]
D_t	0.15	[m]
A_s	1.27	[m^2]
A_t	1.57×10^{-3}	[m^2]
h_s	6.75	[kW/m^2 °C]
h_t	9.20×10^{-1}	[kW/m^2 °C]
d_t	1×10^{-2}	[m]
d_s	1×10^{-2}	[m]
R_{ts}	2.11	[kW/m^2 °C]
Δl	1.80	[m]

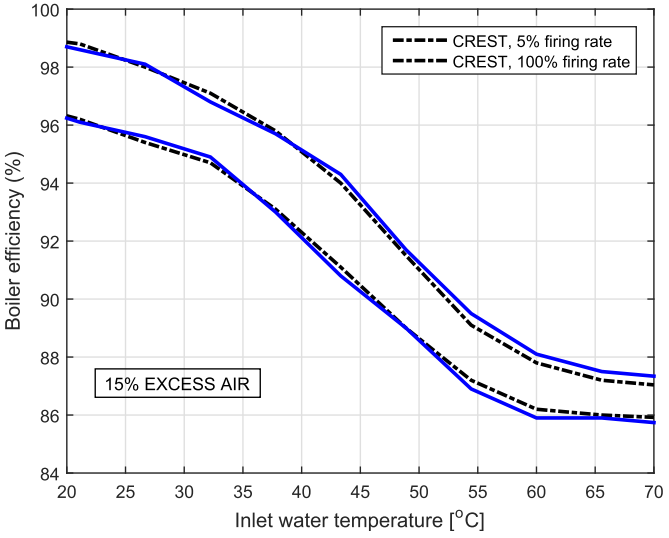

Fig. 6. CREST vs proposed model (with 7 sections).

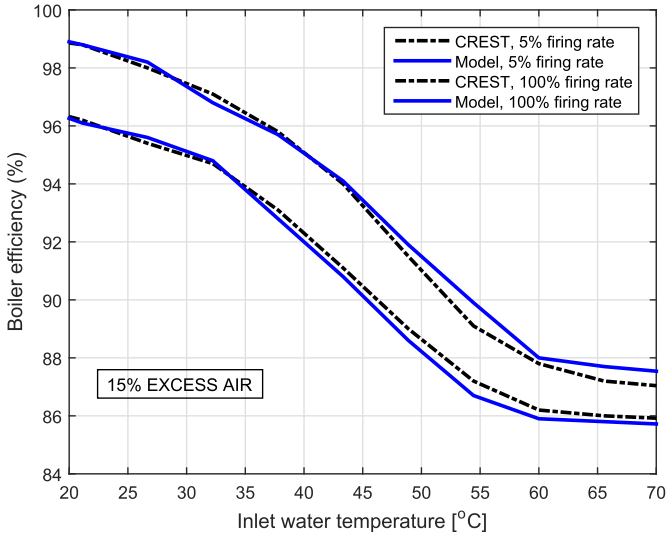

Fig. 5. CREST vs proposed model (with 5 sections).

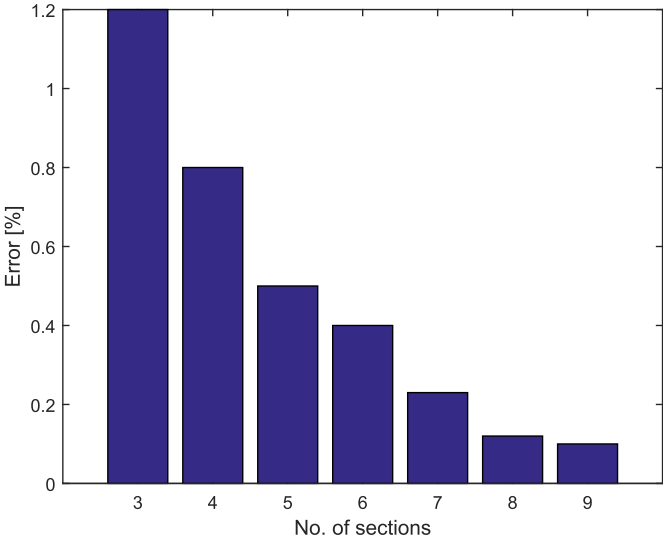

Fig. 7. Model accuracy as function of sections.

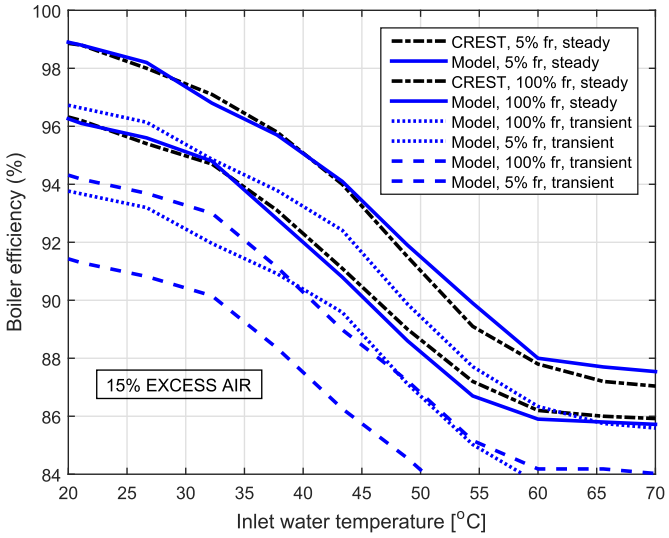

Fig. 8. Transient efficiency curve against steady-state efficiency curve.

approach is a monitoring procedure over the entire dynamic operating range of the boiler: in particular, the two transient efficiency curves in Fig. 8 are calculated from (20) in two instants of time before the steady-state is reached. In order to show the effect of degradations on the efficiency curve, we decrease the nominal h_i, h_o and R_{tf} in Table 2, and plot again the efficiency curves with such values. Fig. 9 shows that the performance curve is indeed degraded with respect to the nominal one in Fig. 5, thus indicating that the proposed model can be used to monitor efficiency degradation. Only steady-state degradation is shown in Fig. 9 for better visibility.

5. Conclusions

Developing accurate and dynamic models of condensing boilers is a key enabler to energy efficiency via better controls and monitoring strategies. In contrast with the state of the art, where model-based monitoring algorithms for energy efficiency are on simplified nonlinear efficiency curves calculated at static (or quasi-stationary) regimes, in this work we proposed a novel monitoring algorithm relying on a hybrid dynamic first-principle modelling. Because of the fact that such model accounts for dynamic heat transfer phenomena and for a time-varying distribution of condensing/non condensing heat exchange, dynamic monitoring of the energy efficiency of condensing boilers during their complete dynamics regime is possible by appropriately designing a set of observers. Interestingly, the proposed approach not only recovers (at steady-state) the static nonlinear efficiency curve, but it also results in a dynamic nonlinear efficiency curve that state-of-the-art approaches cannot provide. The efficiency curve has been shown both in the nominal and degraded case, where degradation in efficiency has been modelled as changes in heat transfer coefficients due to limescale. Comparisons with real-life boiler efficiency data have been presented.

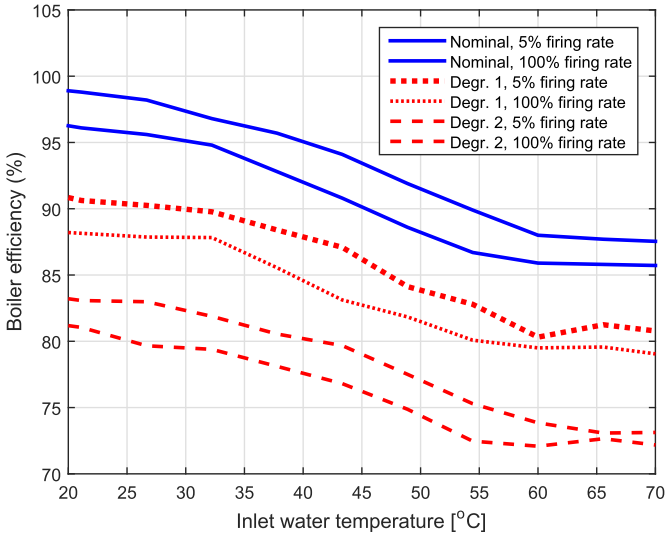

Fig. 9. Efficiency degradation with proposed model (at steady-state).

Acknowledgment

The authors would like to acknowledge Ondrej Holub and Petr Endel from Honeywell Labs for useful discussion about the boiler combustion and operating principles.

References

[1] Pérez-Lombard L, Ortiz J, Pout C. A review on buildings energy consumption information. Energy Build 2008;40(3):394–8.
[2] Cockroft J, Samuel A, Tuohy P. Development of a methodology for the evaluation of domestic heating controls. 2007.
[3] Central Heating System Specifications. Domestic heating by gas: boiler systems - guidance for installers and specifiers. 2008.
[4] Weiss M, Dittmar L, Junginger M, Patel MK, Blok K. Market diffusion, technological learning, and cost-benefit dynamics of condensing gas boilers in The Netherlands. Energy Policy 2009;37(8):2962–76.
[5] Vignali G. Environmental assessment of domestic boilers: a comparison of condensing and traditional technology using life cycle assessment methodology. J Clean Prod 2017;142(Part 4):2493–508.
[6] Seungro L, Sung-Min K, Chang-Eon L. Performances of a heat exchanger and pilot boiler for the development of a condensing gas boiler. Energy 2011;36:3945–51.
[7] Energy Efficiency and Renewable Energy. Building America solution center: condensing boilers. 2015.
[8] Sorensen K. Dynamic boiler performance: modelling, simulating and optimizing boilers for dynamic operation. 2004.
[9] Ternoveanu A, Ngendakumana P. Dynamic model of a hot water boiler. In: Climat 2000 conference, Brussels; 1997.
[10] Sreepradha C, Panda RC, Bhuvaneswari NS. Mathematical model for integrated coal fired thermal boiler using physical laws. Energy 2017;118:985–98.
[11] Sun L, Li D, Lee KY, Xue Y. Control-oriented modeling and analysis of direct energy balance in coal-fired boiler-turbine unit. Control Eng Pract 2016;55:38–55.
[12] Zhang J, Wang N, Wang S. Fuzzy-neuron intelligent coordination control for a unit power plant. Asian J Control 2001;3:57–63.
[13] Zhang Y, He Y, Wu M, Zhang J. Control for discrete-time markovian jump systems with partial information on transition probabilities. Asian J Control 2013;15:1397–406.
[14] Lawrynczuk M. Nonlinear predictive control of a boiler-turbine unit: a state-space approach with successive on-line model linearisation and quadratic optimisation. {ISA} Transactions March 2017;67:476–95.
[15] Lazzarin RM, Schibuola L. Performance analysis of heating plants equipped with condensing boilers. Heat Recovery Sys 1986;6:269–76.
[16] Chen Q, Finney K, Li H, Zhang X, Zhou J, Sharifi V, et al. Condensing boiler applications in the process industry. Appl Energy 2012;89:30–6.
[17] Rosa L, Tosato R. Experimental evaluation of seasonal efficiency of condensing boilers. Energy Build 1990;14:237–41.
[18] Che D, Liu Y, Gao C. Evaluation of retrofitting a conventional natural gas fired boiler into a condensing boiler. Energy Convers Manag 2004;45(20):3251–66.
[19] Barros JP, Azevedo JLT, Monteiro L. Effect of relative humidity in the efficiency of condensing gas water heater appliance. Appl Thermal Eng 2014;65(12):66–73.
[20] Lo Basso G, Nastasi B, G D Astiaso, Cumo F. How to handle the hydrogen enriched natural gas blends in combustion efficiency measurement procedure of conventional and condensing boilers. Energy 2017;123:615–36.
[21] Trojanowski R, Butcher T, Worek M, Wei G. Polymer heat exchanger design for condensing boiler applications. Appl Thermal Eng 2016;103:150–8.
[22] de Oliveira V, Karimi A. Robust and gain-scheduled pid controller design for condensing boilers by linear programming. IFAC Proc Vol 2012;45(3):335–40.
[23] Bojica M, Dragicevic S. Milp optimization of energy supply by using a boiler, a condensing turbine and a heat pump. Energy Convers Manag 2002;43:

591–608.
[24] Baldi S, Le Quang T, Holub O, Endel P. Real-time monitoring energy efficiency and performance degradation of condensing boilers. Energy Convers Manag 2017;136:329–39.
[25] Lemort V, Rodriguez A, Lebrun J. Simulation of hvac components with the help of an equation solver. In: Solar Heating and Cooling Programme International Energy Agency; 2008.
[26] Makaire D, Ngendakumana P. Thermal performance of condensing boilers. In: 32nd TLM-IEA energy conservation and emission reduction in combustion; 2010. p. 1–11.
[27] Aganovic A. Analysis of dynamical behavior of the boiler room at mechanical engineering faculty in sarajevo in standard exploitation conditions. 2013.
[28] Jeong K, Kessen Ml J, Bilirgen H, Levy EK. Analytical modeling of water condensation in condensing heat exchanger. Int J Heat Mass Transfer 2010;53:2361–8.
[29] Satyavada H, Baldi S. A novel modelling approach for condensing boilers based on hybrid dynamical systems. Machines 2016;4:10.
[30] Michailidis I, Baldi S, Pichler MF, Kosmatopoulos EB, Santiago JR. Proactive control for solar energy exploitation: a German high-inertia building case study. Appl Energy 2015;155:409–20.
[31] Seungro L, Sung-Min K, Chang-Eon L. An experimental study of a cylindrical multi-hole premixed burner for the development of a condensing gas boiler. Energy 2011;36:4150–7.
[32] Michailidis I, Baldi S, Kosmatopoulos EB, Boutalis YS. Optimization-based active techniques for energy efficient building control part ii: real-life experimental results. In: International conference on buildings energy efficiency and renewable energy sources, BEE RES; 2014. p. 39–42.
[33] Di Perna C, Magri G, Giuliani G, Serenelli G. Experimental assessment and dynamic analysis of a hybrid generator composed of an air source heat pump coupled with a condensing gas boiler in a residential building. Appl Thermal Eng 2015;76:86–97.
[34] Vigants G, Galindoms G, Veidenbergs I, Vigants E, Blumberga D. Efficiency diagram for district heating system with gas condensing unit. Energy Procedia 2015;72:119–26.
[35] Verhelst C, Logist F, Van Impe J, Helsen L. Study of the optimal control problem formulation for modulating air-to-water heat pumps connected to a residential floor heating system. Energy Build 2012;45:43–53.
[36] Baldi S, Karagevrekis A, Michailidis I, Kosmatopoulos EB. Joint energy demand and thermal comfort optimization in photovoltaic-equipped interconnected microgrids. Energy Convers Manag 2015;101:352–63.
[37] Tzivanidis C, Antonopoulos KA, Gioti F. Numerical simulation of cooling energy consumption in connection with thermostat operation mode and comfort requirements for the athens buildings. Appl Energy 2011;88(8):2871–84.
[38] Satyavada H, Babuska R, Baldi S. Integrated dynamic modelling and multivariable control of hvac components. In: 15th European Control Conference, Aalborg, Denmark, June 29th - July 1st; 2016. p. 1171–6.
[39] Flagan RC, Seinfeld JH. Fundamentals of air pollution engineering. 1 edition. Englewood Cliffs, New Jersey: Prentice Hall; 1988.
[40] Underwood CP, Yik FWH. Modelling methods for energy in buildings. 1 edition. Blackwell Publishing Ltd; 2004.
[41] Gilman GF. Boiler control systems engineering. International society of automation. 2 edition 2010.
[42] Day AR, Ratcliffe MS, Shepherd K. Heating systems, plant and control. 1 edition. Wiley-Blackwell; 2003.
[43] Energia Switched On. Energy efficiency: gas heating in commercial premises. 2016.
[44] Ioannou P, Fidan B. Adaptive control tutorial. Society for industrial and applied mathematics. 1 edition 2006.
[45] Chatterjee S, Sadhu S, Ghoshal TK. Fault detection and identification of nonlinear hybrid system using self-switched sigma point filter bank. IET Control Theory Appl 2015;9(7):1093–102.
[46] Baldi S, Yuan S, Endel P, Holub O. Dual estimation: constructing building energy models from data sampled at low rate. Appl Energy 2016;169:81–92.
[47] Paoletti S, Juloski A Lj, Ferrari-Trecate G, Vidal R. Identification of hybrid systems a tutorial. European J Control 2007;13(2):242–60.
[48] Bako L. Identification of switched linear systems via sparse optimization. Automatica 2011;47(4):668–77.
[49] Narendra KS, Balakrishnan J. Adaptive control using multiple models. IEEE Trans Autom Control 1997;42(2):171–87.
[50] Hespanha JP, Liberzon D, Morse AS. Hysteresis-based switching algorithms for supervisory control of uncertain systems. Automatica 2003;39(2):263–72.
[51] Baldi S, Ioannou PA, Kosmatopoulos EB. Adaptive mixing control with multiple estimators. Int J Adaptive Control Signal Process 2012;26(8):800–20.
[52] Cengel Y, Boles M. Thermodynamics: an engineering approach. 8 edition. McGraw-Hill Education; 2014.
[53] Green Shoots Controls. http://www.greenshootscontrols.net/?p=153.
[54] Lochinvar. Crest condesing boiler. http://www.lochinvar.com/products/default.aspx?type=productline&lineid=177.

List of symbols

T_g: combustion gas temperature
T_w: water temperature
T_t: tube wall temperature
T_s: extended surface temperature
w_g: combustion gas mass flow rate
w_w: water mass flow rate
ρ_g: combustion gas density
ρ_w: water density
ρ_t: tube wall density
ρ_s: extended surface density
c_g: combustion gas specific heat capacity
c_w: water specific heat capacity
c_t: tube wall specific heat capacity
c_s: ext. surface specific heat capacity
D_s: perimeter heat transfer surf. (gas side)
D_t: perim. heat transfer surface (water side)
A_s: effective free flow area (gas side)
A_t: effective free flow area (water side)
h_s: convection coefficient (gas side)
h_t: convection coefficient (water side)
d_s: extended surface thickness
d_t: tube wall thickness
R_{ts}: thermal resistance tube-ext. surface
W_{heat}: latent heat flow